

# Kolmogorov-Sinai Entropy-Rate vs. Physical Entropy

Vito Latora\* and Michel Baranger\*\*

Center for Theoretical Physics, Laboratory for Nuclear Sciences and Department of Physics,  
Massachusetts Institute of Technology, Cambridge, Massachusetts 02139, USA

MIT CTP#2751

chao-dyn/9806006

This letter elucidates the connection between the KS entropy-rate  $\kappa$  and the time evolution of the physical or statistical entropy  $S$ . For a large family of chaotic conservative dynamical systems including the simplest ones, the evolution of  $S(t)$  for far-from-equilibrium processes includes a stage during which  $S$  is a simple linear function of time whose slope is  $\kappa$ . The letter presents numerical confirmation of this connection for a number of chaotic symplectic maps, ranging from the simplest 2-dimensional ones to a 4-dimensional and strongly nonlinear map.

05.45.+b, 05.70.Ln

This paper tries to clarify the connection between the Kolmogorov-Sinai entropy and the physical entropy for a chaotic conservative dynamical system. This connection is obviously very important if one is to understand the impact on thermodynamics and statistical mechanics of the large amount of work done by mathematicians on the behavior of chaotic systems. To start with the KS entropy, it is not really an entropy but an entropy per unit time, or an “entropy-rate”. It is a single number  $\kappa$ , which is a property solely of the chaotic dynamical system considered. As for the physical entropy  $S(t)$ , the entropy of the second law of thermodynamics, it is a function of time, and this function depends not only on the particular dynamical system, but also on the choice of an initial probability distribution for the state of that system. Though it is clear that the original definition of  $\kappa$  [1] was meant to provide a connection with  $S(t)$ , the precise connection does not seem to be well known nowadays, and the few statements found in the textbooks are often vague [2].

The simplest connection one might guess would be this: the KS entropy-rate would be the maximum possible absolute value of the rate of variation of the physical entropy, i.e.  $|dS/dt| \leq \kappa$ . But this is wrong, because a counterexample can easily be found [3,4]. The actual connection is less direct and, in many cases, it requires that  $S(t)$  be averaged over many histories (or trajectories), so as to give equal weights to initial distributions from all regions of phase space. Then, assuming these initial distributions to be very far from equilibrium, the variation with time of the physical entropy goes through three successive, roughly separated stages. In the first stage,  $S(t)$  is heavily dependent on the details of the dynamical system and of the initial distribution; no generic

statement can be made;  $dS/dt$  can be positive or negative, large or small, and in particular it can be larger than  $\kappa$ . In the second stage,  $S(t)$  is a linear increasing function whose slope is  $\kappa$ . In the third stage,  $S(t)$  tends asymptotically toward the constant value which characterizes equilibrium, for which the distribution is uniform in the available part of phase space. It may happen, however, that the simple and generic stage 2 is absent, with stages 1 and 3 merging into each other. This is true when the initial distribution is not sufficiently different from the equilibrium distribution.

We make no claim of having a rigorous mathematical proof of these statements. We do have an incomplete, but quite suggestive, analytical discussion [3], which cannot fit in the space available here. The latter part of this letter will present a few very convincing numerical simulations for symplectic maps of 2 and 4 dimensions. Ref. [3] contains more map results, as well as a 3-dimensional flow. Some of our ideas are already present in ref. [5], including the three-stage idea; but the crucial connection with the KS entropy-rate, valid for any number of dimensions and for nonlinear systems, is not there. Note that the definition of a single global  $\kappa$  is not always a useful one, for instance for several weakly coupled subsystems; in such cases the connection clearly needs generalization.

The definition of the KS entropy-rate can be found in many textbooks [6]. To calculate it here, we use the fact that it is equal to the sum of the positive Lyapunov exponents [7]. Our definition for the out-of-equilibrium physical entropy is  $S = \text{constant} - I$ , where  $I$  is the Shannon information [8]. These  $S$  and  $I$  are coarse grained [9]. Coarse-graining consists in performing a slight smearing, or smoothing, of the probability distribution in phase space before calculating  $S$  or  $I$ . The fine-grained quantities do not vary with time at all, because Liouville’s theorem says that the volume of phase space is conserved. The shape of that volume, however, becomes increasingly complicated and fractalized, due to the chaotic dynamics. Hence, under smoothing, the volume occupied keeps increasing. There are many ways to perform a coarse-graining. For this paper, we assume that phase space is divided into a large number of cells  $c_\alpha$  with volumes  $v_\alpha$ , such that  $\sum_\alpha v_\alpha = V$ , the total volume of available phase space. Then we define  $I$  by

$$I(t) = \sum_\alpha p_\alpha(t) \log \left[ \frac{V}{v_\alpha} p_\alpha(t) \right] , \quad (1)$$

where  $p_\alpha(t)$  is the probability that the state of the system in phase space at time  $t$  falls inside cell  $c_\alpha$ . In the following it will be more convenient to work with  $I(t)$  rather than  $S(t)$ . This is because, when  $I$  is used, there is a convenient reference point, the uniform distribution, whose  $I$  always vanishes, irrespective of the coarse-graining. On the other hand the constant quantity  $I+S$ , and therefore  $S$ , do depend on the coarse-graining.

This type of coarse-graining allows an alternative version of the significance of  $\kappa$  for the evolution of a physical system. Let us assume the initial distribution to be very strongly localized in phase space, i.e. most cells contain zero probability initially. Then, during the generic “second stage” mentioned earlier, the total number of occupied cells, i.e. cells with non-vanishing  $p_\alpha$ , varies proportionally to  $e^{\kappa t}$ . Our simulations verify this fact well (see fig. 3 later).

We return to the need for averaging, in our simulations, many histories starting from different parts of phase space. This has to be done whenever the local  $\kappa$  (the sum of the positive local Lyapunov exponents) varies appreciably from place to place, which is the normal case for nonlinear systems. For linear maps (like the generalized cat map below) it is not necessary. For other systems, it would never be necessary if we could use a fine enough coarse-graining, to give the probability time to spread throughout phase space before any appreciable increase in entropy. Unfortunately such fine grain would require computers far more powerful than exist now. In the real thermodynamical world with many many dimensions, what kind of coarse-graining should preferably be used is, we believe, a wide open question.

For what may be the simplest of all conservative chaotic systems, the baker’s map, the correctness of our three-stage description for the behavior of  $I(t)$  can be shown analytically [3]. Our first simulations are done with the “generalized cat map” inside a unit square:

$$\begin{aligned} P &= p + kq \pmod{1}, \\ Q &= p + (1+k)q \pmod{1} \end{aligned} \quad (2)$$

where  $k$  is a positive control parameter. Fig. 1 shows  $I(t)$  for four values of  $k$  (see caption). The coarse-graining grid is obtained by dividing each axis into 400 equal segments. The initial distribution consists of  $10^6$  points placed at random inside a square whose size is that of a coarse-graining cell, and the center of that square is picked at random anywhere on the map. Each of the four curves is an average over 100 runs, i.e. 100 histories with different initial distributions chosen at random, as mentioned. Each curve shows clearly the stage-2 linear behavior, the negative of the slope being accurately given by the (analytically calculable) Lyapunov exponent:

$$\lambda = \log \frac{1}{2}(2 + k + \sqrt{k^2 + 4k}) = \kappa \quad . \quad (3)$$

Fig. 2 shows how  $I(t)$  depends on the initial distribution and on the coarse-graining. Now  $k = 1$  only. Other conditions are the same as in fig. 1, except that we calculate a single history instead of averaging 100. This makes no big difference in this case, because the local Lyapunov exponent is the same everywhere. In the six top curves six different sizes are compared for the initial square; the grid is as in fig. 1. The first size is that of 1 coarse-graining cell, then 4 cells, 16, 64, 256, and 1024 cells (from top to bottom). All six curves have the same stage-2 slope given by  $-\kappa$ . Their vertical displacement is  $\log 2$  for each factor 2 in the linear dimension of the initial distribution. The three bottom curves show how  $I(t)$  depends on the coarse-graining. The size of the initial square is always that of 1024 original coarse-graining cells. For the upper curve (sixth from the top) the cells are as in fig. 1, for the middle curve they are squares four times larger in area, and for the bottom curve they are four times larger again. Once again, all three curves have the same stage-2 slope of  $-\kappa$ . They are displaced vertically from each other by the log of the factor in coarse-graining linear dimension, i.e.  $\log 2$ .

In fig. 3 we plot on a log scale the number of occupied cells vs. time for the finest coarse-graining and 3 progressively larger initial distributions, whose centers are picked at random as always. All 3 stage-2 straight lines are indeed fitted by  $e^{\kappa t}$ . Their vertical displacement is by a factor 4, which is also the factor in the linear size of the initial distributions.

The second system studied is the standard map [10], again a two-dimensional conservative map in the unit square, but this time nonlinear:

$$\begin{aligned} P &= p + \frac{k}{2\pi} \sin(2\pi q) \pmod{1}, \\ Q &= q + P \pmod{1}. \end{aligned} \quad (4)$$

The map is only partially chaotic, but the percentage of chaos increases with the control parameter  $k$ , and we use large values of  $k$ , namely 20, 10, and 5. For  $k = 5$  there are two sizeable regular islands, associated with a period 2 stable trajectory. We calculated the Lyapunov exponent numerically, leaving out the regular islands for  $k = 5$ . This yielded  $\lambda = \kappa = 2.30, 1.62, 0.98$ , respectively for the three  $k$ ’s. Fig. 4 shows the three curves  $I(t)$ , with the top curve corresponding to the smallest  $k$ . The coarse-graining grid, the choice of initial distribution, and the averaging are the same as for fig. 1, but it was necessary to include 1000 histories in the averaging for  $k = 5$ . Each curve has a stage-2 linear portion whose slope is correctly given by  $-\kappa$ . Fig. 5 presents 3 single histories (x’s) for  $k = 5$ , as well as the average curve from fig. 4 (circles). For such a very nonlinear system, with too coarse a grain, the single curves vary wildly and the averaging is essential.

Our next example is a four-dimensional system, a generalized cat map. It is a linear symplectic map

[11], reduced to a unit-size hypercube by introducing “mod 1” in each of the four transformation equations. The two positive Lyapunov exponents  $\lambda_1$  and  $\lambda_2$  can be calculated analytically, and the KS entropy-rate is  $\kappa = \lambda_1 + \lambda_2$ . For this system we made up the coarse-graining grid by dividing each of the four axes into 20 equal segments. The initial distribution consists of  $10^6$  points placed at random inside one hypercube of size  $(400)^{-1} \times (400)^{-1} \times (400)^{-1} \times (400)^{-1}$ , and the center of the hypercube is picked at random anywhere on the map. Fig. 6 shows  $I(t)$  for 2 single histories. They differ greatly in their stage 1, but both have nearly linear stage 2’s with the correct slope given by  $-\kappa$ .

Finally we have a 4-dimensional nonlinear map, made up of two coupled standard maps :

$$\begin{aligned} P_1 &= p_1 + \frac{k_1}{2\pi} \sin(2\pi q_1) \pmod{1} \\ Q_1 &= q_1 + P_1 + mP_2 \pmod{1} \\ P_2 &= p_2 + \frac{k_2}{2\pi} \sin(2\pi q_2) \pmod{1} \\ Q_2 &= q_2 + P_2 + mP_1 \pmod{1}. \end{aligned} \quad (5)$$

We worked with 3 sets of control parameters  $(k_1, k_2)$ , namely (10,5), (5,3), and (3,1). The coupling parameter  $m$  was 0.5 in all cases. We calculated the two Lyapunov exponents numerically [12], then added them up to get  $\kappa$ . The numerical values are in the figure caption. The initial volume was the size of one cell, and we averaged over 100 histories. Fig. 7 shows  $I(t)$ . It has a fairly well defined second stage with a slope close to  $-\kappa$  in all cases.

The work we have reported makes very explicit the connection between the KS entropy-rate, when it is meaningful, and the time dependence of the physical entropy or information. Yet it is far from a complete answer. It assumes that, at the beginning of the system’s evolution, the probability distribution spreads very fast to all corners of phase space before undergoing much fractalization, so that its subsequent variation is well described by a global  $\kappa$ . But there are other possible scenarios. For instance there may be gradual overall evolution in space as well as in time, a possibility which is not included by our assumption that all parts of phase space must start on an equal footing. In conclusion, although this work constitutes only a quick foray into the subject, we hope that our assertions can function as guiding principles for research attempting to bring together the mathematics of chaos and the physics of far-from-equilibrium thermodynamics.

#### ACKNOWLEDGMENTS

We thank A. D’Andrea, A. Rapisarda, and M. Saraceno for fruitful discussions. Also S. Ganguli and B. Müller who furnished some pointers to the literature. Financial support was provided by INFN (for V. L.), and at

MIT by the U.S. Department of Energy (D.O.E.) under contract #DE-FC02-94ER40818.

\* E-mail: latora@ctp.mit.edu

\*\* E-mail: baranger@ctp.mit.edu

- [1] A. N. Kolmogorov, Dokl. Akad. Nauk SSSR **119**, 861 (1958); **124**, 754 (1959).
- [2] Perhaps the most explicit is on p. 39 of G. M. Zaslavsky, *Chaos in Dynamic Systems*, Harwood, Chur (1985).
- [3] M. Baranger, M. Girvan, N. Krishnaswami, V. Latora, and J. Ogrzydziak, in preparation.
- [4] N. Krishnaswami, *Some Theorems about the Kolmogorov-Sinai Entropy and its Use in Thermodynamics*, B.Sc. Thesis, M.I.T., May 1997.
- [5] Y. Gu, J. Wang, Phys. Lett. **A229**, 208 (1997).
- [6] For instance P. Billingsley, pp. 61 and 84 in *Ergodic Theory and Information*, Wiley, New York (1965).
- [7] Ya. B. Pesin, Russian Math. Surveys **32:4**, 55 (1977).
- [8] R. Balian, sec. 3.1 in *From Microphysics to Macrophysics*, vol. I, Springer-Verlag, New York (1991).
- [9] R. Balian, *loc. cit.* p. 135.
- [10] M. Tabor, sec. 4.2.e in *Chaos and Integrability in Non-linear Dynamics*, Wiley, New York (1989).
- [11] V. I. Arnold, *Mathematical Methods of Classical Mechanics*, Springer-Verlag, New York (1978).
- [12] G. Benettin, L. Galgani, A. Giorgilli, and J.M. Strelcyn, *Meccanica* **9**, 21 (1980); A. Wolf, J. Swift, H. Swinney, and J. Vastano, *Physica* **D16**, 285 (1985).

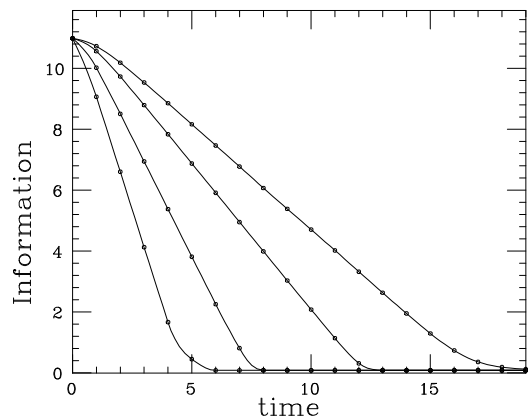


FIG. 1. Generalized Cat Map,  $k = 10, 3, 1, 0.5$  (from left to right),  $\kappa = 2.48, 1.57, 0.96, 0.69$  respectively,  $N = 10^6$ , grid =  $400 \times 400$ ,  $V_i = V_{\text{cell}}$ , average of 100 histories.

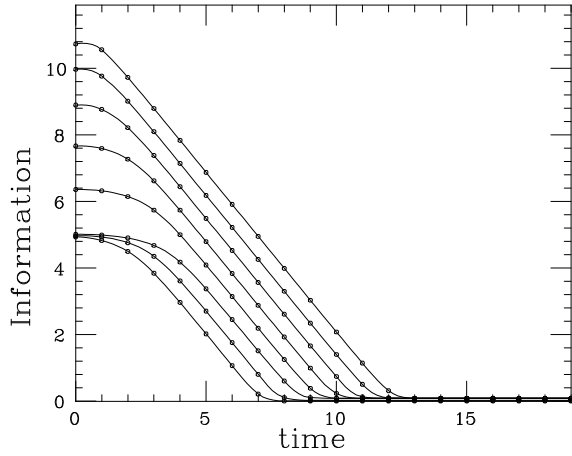


FIG. 2. Generalized Cat Map,  $k = 1, \kappa = 0.96, N = 10^6$ ; from top to bottom: grid =  $400 \times 400, V_i/V_{\text{cell}} = 1, 4, 16, 64, 256, 1024$  (six curves), and grid =  $200 \times 200, 100 \times 100, V_i/V_{\text{cell}} = 1024$  (two curves), 1 history.

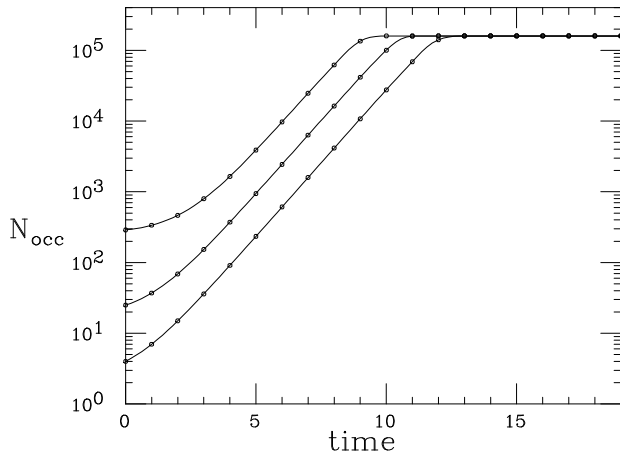


FIG. 3. Generalized Cat Map,  $k = 1, \kappa = 0.96, N = 10^6$ , grid =  $400 \times 400, V_i/V_{\text{cell}} = 1, 16, 256$  (bottom to top), 1 history.

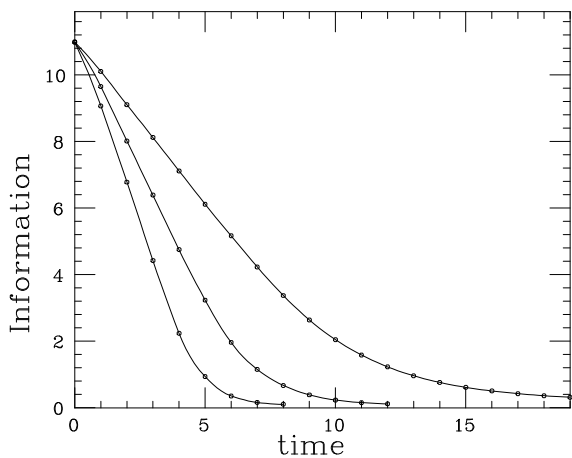


FIG. 4. Standard Map,  $k = 20, 10, 5$  (from left to right),  $\kappa = 2.30, 1.62, 0.98$  respectively,  $N = 10^6$ , grid =  $400 \times 400, V_i = V_{\text{cell}}$ , average of 100 hist. ( $k = 20, 10$ ), 1000 hist. ( $k = 5$ ).

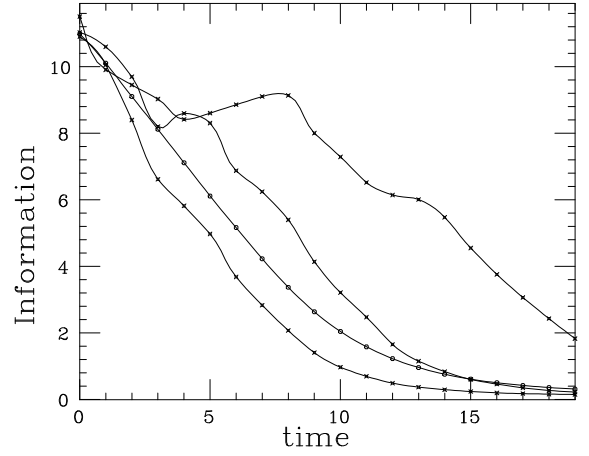


FIG. 5. Standard Map,  $k = 5, \kappa = 0.98$ , 3 single histories compared with the average from fig. 4.

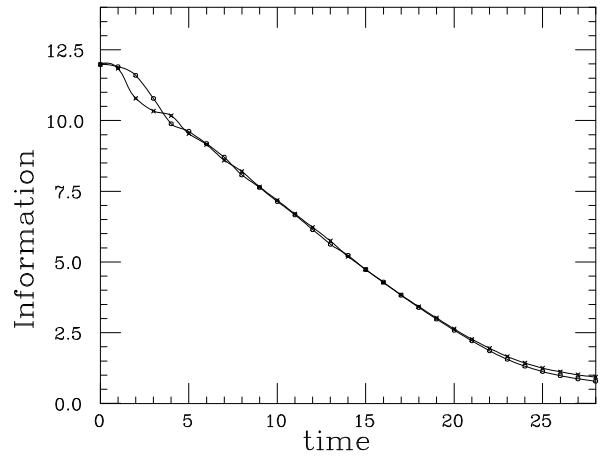


FIG. 6. 4-Dimensional Generalized Cat Map,  $\lambda_1 = 0.223, \lambda_2 = 0.247, \kappa = 0.470, N = 10^6$ , grid =  $20^4, V_i = (20)^{-4} V_{\text{cell}}$ , 2 single histories.

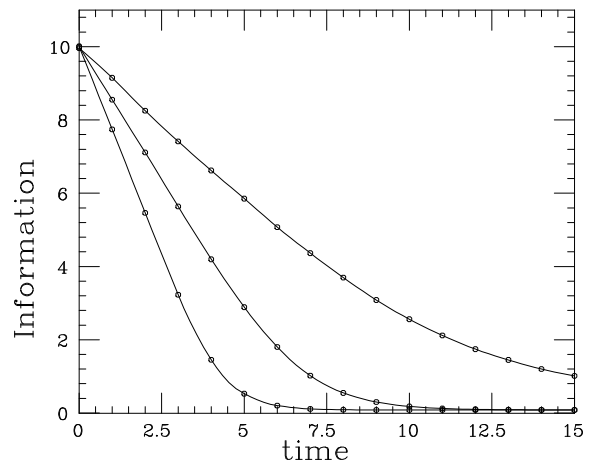


FIG. 7. 4-Dimensional Nonlinear Map. Bottom:  $k_1 = 10, k_2 = 5, m = 0.5, \lambda_1 = 1.65, \lambda_2 = 0.75, \kappa = 2.40$ . Middle:  $k_1 = 5, k_2 = 3, m = 0.5, \lambda_1 = 1.03, \lambda_2 = 0.45, \kappa = 1.48$ . Top:  $k_1 = 3, k_2 = 1, m = 0.5, \lambda_1 = 0.62, \lambda_2 = 0.16, \kappa = 0.78$ .  $N = 10^6$ , Grid =  $20^4, V_i = V_{\text{cell}}$ , average of 100 histories.